

RIGA TECHNICAL UNIVERSITY

Faculty of Material Science and Applied Chemistry

Institute of Silicate Materials

Andris ŠUTKA

PhD student of Doctoral study programme “Chemical Technology”

**PHYSICAL PROPERTIES OF
NANOSTRUCTURED NICKEL ZINC
FERRITES SYNTHESIZED BY SOL-GEL
METHOD**

Summary of Doctoral Thesis

Scientific supervisor

Dr. Habil. Sc. Eng., Professor

Gundars MEŽINSKIS

Riga 2012

Šis darbs izstrādāts ar Eiropas Sociālā fonda atbalstu projektā «Atbalsts RTU doktora studiju īstenošanai».

This work has been supported by the European Social Fund within the project “Support for the implementation of doctoral studies at Riga Technical University”.

Эта работа выполнена при содействии Европейского социального фонда в рамках проекта «Поддержка развития докторантуры РТУ».



THE DOCTORAL DISSERTATION IS PROMOTED TO
BE DEFENDED FOR THE DOCTORAL DEGREE IN PHYSICS
AT RIGA TECHNICAL UNIVERSITY

The doctoral dissertation for the doctoral degree in Chemical Engineering will be defended at 14:00 o'clock on December 6 2012 at Riga Technical University, Faculty of Material Science and Applied Chemistry, Riga Azenes Street 14/24, Room No. 272.

OFFICIAL OPPONENTS

Dr.habil.sc.ing., Assoc. Profesors Visvaldis Švinka
Riga Technical University, Institute of Silicate Materials

Dr.habil.phys., Profesors Ivars Tāle
University of Latvia, Institute of Solid State Physics

Dr.phys., Kristjan Saal
University of Tartu, Institute of Physics

APPROVAL

With the following I approve that I've elaborated current doctoral dissertation, which is submitted to be reviewed in Riga Technical University to qualify for the doctoral degree in Physics and doctoral dissertation is not submitted anywhere else to qualify for a scientific degree.

Andris Šutka _____ (signature)

Date _____

Table of contents

OVERALL REVIEW OF THE THESIS.....	5
Introduction.....	5
The state of art	6
Aims.....	6
Scientific novelty	6
Composition and volume of the thesis	7
Approbation and publication of the thesis.....	7
CONTENTS OF THE THESIS	8
Review of literature	8
Methods	9
Results.....	12
Overall conclusions	30
STATEMENTS TO DEFEND	31
REFERENCES	31
LIST OF AUTHOR PUBLISHED PAPERS	32
Articles in journals and scientific proceedings.....	32
Patents.....	33
Conference theses	33

OVERALL REVIEW OF THE THESIS

Introduction

Ni-Zn spinel type ferrites are interesting materials due to their both magnetic and semiconductor properties. These materials are widely used and exploited already from the 50ties of the last century. Nowadays, the use of the ferrite materials grows and, continuing miniaturization trend in electrical engineering, there is a need to develop synthesis methods and to do characterization of the ferrite nanomaterials. Moreover, the variety of ferrite applications grows. For example, spinel ferrites due to their transition metal semiconductor properties in the last decade are found to be used as gas sensor materials.

With an increasing need in gas detection for environmental monitoring purposes, such as industrial process control, the use of gas sensors increases. First, it should be known, that as gas sensors can be used materials with high specific surface area – nanomaterials. Also, the semiconductor gas sensors should have fast response behaviour, low response to environmental humidity, high selectivity and long term stability. A material which has all mentioned properties does not exist; thus, searching for new materials or modifying the possibilities of the existing materials is still a topical problem. For example, SnO_2 as a gas sensor material is used already from 1962, but in the field of gas sensors, investigations regarding its modification possibilities are still continuing. The optimisation ways of the spinel type ferrite gas sensor materials are in the starting position. By analysing the literature on the subject, it can be concluded that there is no attention paid to the influence of the charge carrier (point defect) concentration on ferrite gas sensitivity. It is known that electric conductivity is directly connected with metal oxide semiconductor gas sensor sensitivity; thus, in the current PhD work attention first and foremost is paid to the investigation of the electrical properties of Ni-Zn ferrite nanomaterials.

In accordance with the above mentioned the main attention is paid to the synthesis of Ni-Zn ferrite nanomaterials, as well as to the investigation of electric, dielectric and gas sensing properties. In general, the work can be divided into five parts. In the first part attention is paid to the Ni-Zn ferrite synthesis by sol-gel auto combustion (SGAC), in the second part - to the investigation of the influence of composition and stoichiometry on the physical properties of nanostructured Ni-Zn ferrites. The third part is devoted to the influence of the processing temperature on the physical properties of Ni-Zn ferrites. The fourth part is dedicated to the synthesis and properties of nanostructured Ni-Zn ferrite thin films and the last, fifth part, is meant for the investigation of Ni-Zn ferrite gas sensitivity.

The state of the art

It is known, that the electric properties of Ni-Zn ferrites are influenced by composition, stoichiometry and microstructure. It is also known that the change of electric and dielectric properties with zinc content for microstructured Ni-Zn ferrites is different from that of nanostructured ones. There is no equipollent information about the reasons for adjustment of electric and dielectric properties of the nanostructured Ni-Zn ferrites in literature. There is also no information about electric and dielectric properties of nanostructured non-stoichiometric, as well as microstructured stoichiometric and non-stoichiometric Ni-Zn ferrites derived from nanoparticles. In spite of that, there is a tendency of miniaturization in the electronic industry. However, only few research papers can be found on the properties of Ni-Zn ferrite thin films (2D nanomaterials) or their synthesis by spray pyrolysis. Also, there is no attention paid to the influence of charge carrier (point defect) concentration on spinel type ferrite gas sensor sensitivity. A purposeful research on electric and gas sensing properties is believed to hold significant information about nanostructured Ni-Zn ferrites.

Aims

1. To estimate the influence of zinc content on the nanostructured Ni-Zn ferrite electric and dielectric properties.
2. To explore the influence of iron ion stoichiometry on the electric and dielectric properties of nanostructured and microstructured Ni-Zn ferrites derived from nanoparticles.
3. To assess the influence of zinc content on the nanostructured Ni-Zn ferrite gas sensing properties.
4. To find possible ways for the improvement of gas sensing properties of Ni-Zn ferrites.
5. To derive and realize practically a model which will allow assessing the reasons for the change of the obtained Ni-Zn ferrite gas sensor sensitivity by the use of impedance spectroscopy.
6. To develop a functional, integrable gas sensor with an elevated sensitivity, in which a nanostructured 2D ferrite material is used as an active element.

Scientific novelty

The novelty of the work is connected with the synthesis of nanostructured Ni-Zn ferrite electroceramics, the investigation of its properties and clarification of its influencing factors. As the latest research papers and European Union calls of the 7th Framework projects demonstrate, there is a necessity for the synthesis and development of novel nanostructured gas sensitive oxide materials; the main attention is paid to synthesis and the investigation of nanostructured Ni-Zn ferrite gas sensor materials.

Relatively small number of studies is found in literature on the development and investigation of spinel type ferrite gas sensors, as well as there is no information and no attention paid to the influence of charge carrier or point defect concentration on sensitivity of these materials.

The practical significance of the work is determined by the elaboration of a new method based on impedance spectroscopy, which can be used to evaluate the change of sensitivity of the obtained ferrite gas sensor materials, as well as that by the use of the obtained results miniaturized 2D ZnFe₂O₄ nanomaterial with high sensitivity has been made.

The practical use of gas sensors is possible in different areas, for example, in medical diagnosis, food industry, air quality monitoring, for the detection of toxic, flammable and explosive gases, to oversee biotechnological processes, control combustion emissions, and for the monitoring of industrial processes to improve product quality.

Composition and volume of the thesis

The 173 pages of the dissertation, including 129 pictures and 22 tables, comprise the introduction and 5 chapters: a review of literature, methodological part, experimental part, overall conclusions and the statements to defend, a list of papers published by the author, and a list with 207 references.

Approbation of the thesis

Results presented in the dissertation are approbated in 16 peer-reviewed journal articles (10 of them SCI), 14 conference proceedings and have been protected by 2 patents of Latvia.

CONTENTS OF THE THESIS

Review of literature

The section includes the analysis of published literature data. Problems with regard to crystal structure, solid solutions, properties and applications of spinel ferrites were reviewed. Ferrite and ferrite nanomaterial synthesis methods were reviewed, with particular attention to the sol-gel auto-combustion synthesis method. As the last but not less important part of literature data review was devoted to metal oxide semiconductor gas sensors, their operation principles and the role of different factors on their properties, as well as modification possibilities were reviewed.

To summarize, it can be concluded, that spinel type ferrites, especially Ni-Zn ferrites, are the materials with wide application possibilities. By changing ratio between nickel and zinc ion in Ni-Zn ferrites or by making non-stoichiometric compounds, it is largely possible to influence magnetic and electric properties of ferrites.

As Ni-Zn ferrites are transition metal oxide semiconductors, their charge carrier concentration and electrical conductivity is mainly influenced by the quantity of metal ion pairs with different valence or the concentration of oxygen or cation vacancies. The microstructure of the polycrystalline ferrites plays also a great role on their transport properties. The hopping type charge transport in spinel ferrites takes place between ions in octahedral crystallographic site. Iron ions provide electron hopping $\text{Fe}^{3+} + e^- \rightarrow \text{Fe}^{2+}$ (n-type), but nickel ions provide hole hopping $\text{Ni}^{2+} + h^+ \rightarrow \text{Ni}^{3+}$ (p-type).

In case of microstructured Ni-Zn ferrites, due to their high processing temperatures (above 1100°C), a high loss of zinc ions occurs, thus increasing the charge carrier (electron) concentration by reducing Fe^{3+} to Fe^{2+} . With increasing zinc ion content the electrical resistance of the microstructured Ni-Zn ferrites decreases. For nanostructured Ni-Zn ferrites by increasing zinc ion content electrical resistance also increases. In literature it is related to the increase of hopping distance or the increase of material homogeneity, which is quite a notional explanation. By turning attention to the research performed in the middle of the 20th century on electrical properties of Ni-Zn ferrites with a high cation vacancy concentration in the octahedral site, it can be concluded, that the resistance increase is due to charge carrier recombination. For the synthesis of nanostructured Ni-Zn ferrites there is no need for high processing temperatures; thus, there is lower loss of zinc ion, which leads to the reduction of Ni^{3+} and not Fe^{3+} ion.

Moreover, it should be mentioned that nanostructured spinel type ferrites in a comparison with microstructured ones have higher electrical resistance, not only due to lower charge carrier concentration, but also due to smaller grain sizes. With decreasing grain size, the specific amount of grain boundaries in the structure increases, which works as barriers to the flow of

charge carriers. From the practical point of view it is very important to get Ni-Zn ferrites with high electrical resistance, as due to increasing resistance eddy current and energy loss decreases.

The ceramic method is the most popular method used for Ni-Zn ferrite materials. This method involves high processing or the sintering temperatures (1100-1400 °C); thus, particle or grain sizes of Ni-Zn ferrites obtained by a conventional method is in size of micrometres. The high processing temperatures also promote zinc volatilization and formation of nonstoichiometric, inhomogeneous compounds. Spinel structure ferrite nanomaterial synthesis methods have a common feature – all reagents are mixed at an atomic or a molecular level; thus, there is no necessity for high annealing temperatures for the formation of monophasic materials. High homogeneity, stoichiometry and small particle size are the characteristic features of ferrite materials synthesized by wet chemical methods. Finer particle size requires much lower sintering temperatures in comparison with the ceramic method. Overall, the sol-gel auto combustion method seems to be the most promising technique for the synthesis of spinel ferrite nanopowders, while spray pyrolysis – for the synthesis of ferrite thin films (2D nanomaterials). Both methods are simple to perform, do not require special equipment or expensive raw materials, and result in high quality ferrite materials.

From the literature review it can be concluded that these spinel type ferrite materials could be considered a new class of gas sensor materials. Earlier reports on the spinel ferrite gas sensors could be found only 10 years ago. The literature review devoted to ferrite gas sensors allowed concluding that researchers did not pay attention to the influence of charge carrier (point defect) concentration on spinel type ferrite gas sensor sensitivity. Authors of previous researches mainly concentrated on the synthesis of specific structures (1D and 2D) or particles as small as possible, as well as verified ferrite sensitivity or compared that with existing materials.

Methods

For the synthesis of $\text{Ni}_{1-x}\text{Zn}_x\text{Fe}_{2+z}\text{O}_4$ (where $x=0; 0,3; 0,5; 0,7; 1$ and $z= -0,025; -0,01; 0; 0,05; 0,1; 0,15; 0,2$) the sol-gel auto combustion was used. Method involves dissolution of metal nitrates and a complexing agent (citric acid) in distilled water and neutralization of the solution by NH_4OH . In the next step the solution was evaporated to obtain xerogel. The combustion reaction of the xerogel was initiated at 250°C. Molar ratio of metal nitrates and citric acid was taken 1:1.

Tablet shaped samples 1mm thick and 10mm in diameter were uniaxial pressed from as-burnt powders applying pressure of 5 MPa. The samples were sintered at temperatures from 800 to 1300°C.

Nanostructured Ni-Zn ferrite ($\text{Ni}_{1-x}\text{Zn}_x\text{Fe}_2\text{O}_4$, where $x=0; 0,3; 0,5; 0,7; 1$) thin films on glass substrate were obtained by using spray pyrolysis. Its schematic representation is shown in Fig. 1, but the processing parameters are shown in Table 1.

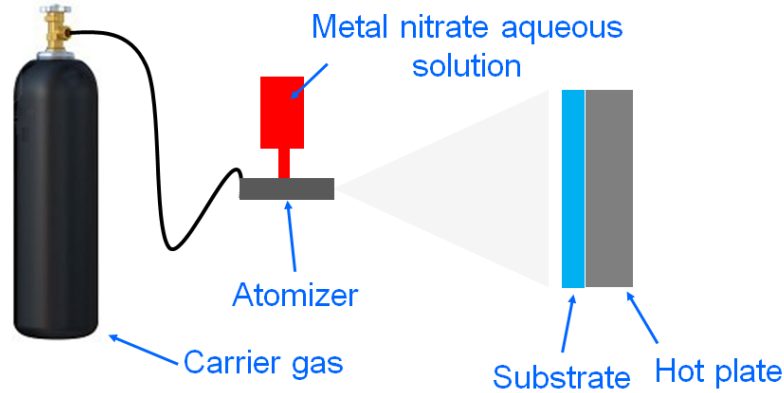


Fig. 1. Schematic representation of spray pyrolysis

Table 1
Experimental parameters of $\text{Ni}_{1-x}\text{Zn}_x\text{Fe}_2\text{O}_4$ thin film spray pyrolysis deposition process

Solution concentration	0,1 M
Substrate temperature	500 °C
Distance to substrate	25 cm
Spray rate	0,4±0,02 ml/s
Carrier gas	nitrogen
Pressure	0,3 MPa
Duration of one spray	0,5 s
Number of cycles	10

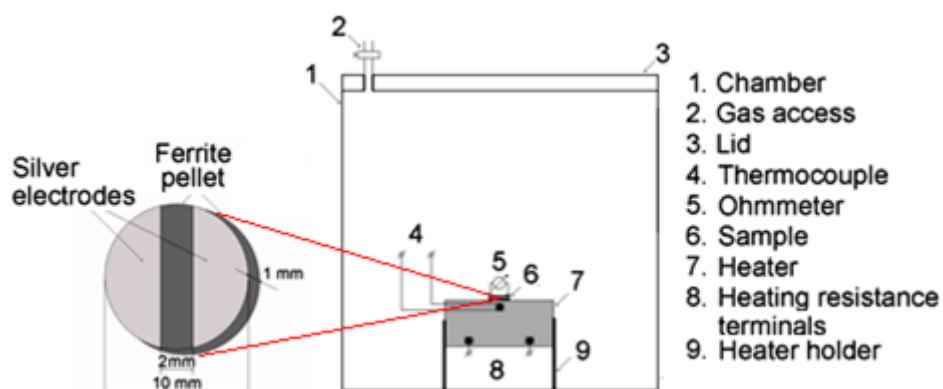


Fig. 2. Schematic representation of experimental gas sensor testing array

Thermogravimetric analysis, BET nitrogen adsorption, Fourier infrared spectroscopy, X-ray diffraction, atomic force microscopy, scanning electron microscopy, energy dispersive X-ray spectroscopy and impedance spectroscopy were used for the characterization of materials. Also, porosity

and density, Fe^{2+} content, electrical resistance, gas sensitivity, magnetic and optical property measurements were performed. Two types of measurement complexes for gas sensing measurements were made. For gas sensing measurements on pellet shaped sample surface electrodes were applied as shown in Fig. 2. In one case measurement complex consisted of a self-made 3000 cm^3 Teflon camera and several auxiliary devices (Fig. 2), but in the second case, for sensitivity measurements at low concentration it was made from measurement complex consisting of a huge polypropylene camera (156 l) and a floodgate (Fig. 3) with sitting sensor element and electrical connections.

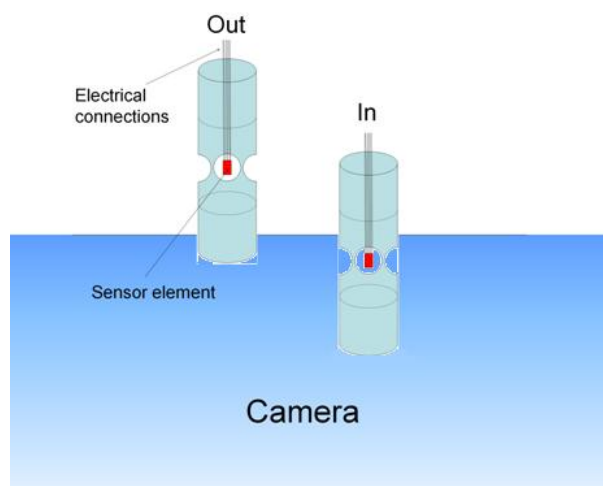


Fig. 3. Schematic view of the sample movement “in” and “out” of the test chamber

Ferrite thin film gas sensors were made by spray pyrolysis on a commercially available multi sensor platform Heraeus MSP 632 (Germany) the size of which is $3.2 \times 6.1 \text{ mm}$ and with integrated Pt electrodes, a Pt1000 temperature sensor, and a heater (see Fig. 4).

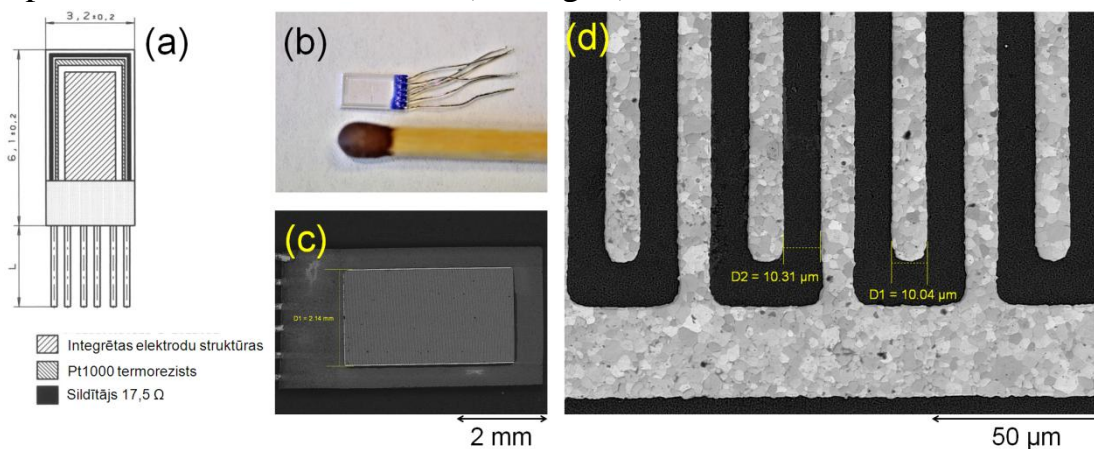


Fig. 4. Commercial sensor platform for thin ferrite film gas sensor testing: (a) schematic view, (b) digital photography, (c) and (d) SEM microphotographs at different magnifications

Influence of the presence of volatile organic compounds in the air on the electric properties of different phases of a sensor material was evaluated by the use of impedance spectroscopy. Test fixture HP 16047B with a self-provided heater, sample holder and electrical connections was used for the measurements. To control temperature, the heater was provided with chromel-alumel thermocouple. Electrical properties of different phases were calculated by fitting equivalent circuit to complex impedance spectra by using the Zview2 software.

Results

Self-ignition reaction temperatures of the xerogels, which correspond to respective ferrites, were determined by means of thermogravimetry (TG). During the auto combustion reaction the process of oxide formation involved the liberation of gaseous products, which was accompanied by a decrease of mass (Fig. 5). Auto combustion self-ignition temperatures for different xerogels were $\sim 200^\circ\text{C}$.

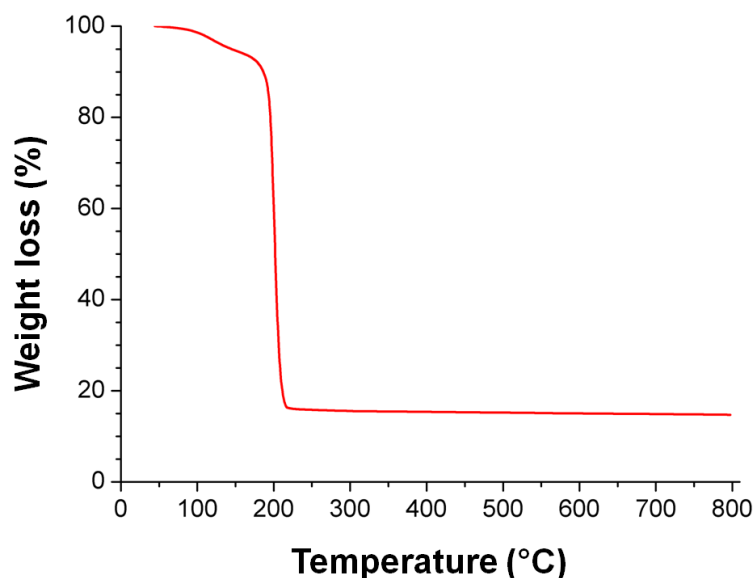


Fig. 5. TG curve of NiFe₂O₄ xerogel

In SEM microphotographs of auto combustion reaction the powder-like products demonstrate that they consist of porous particle aggregates (Fig. 6 (a) and (b)). At a higher magnification (Fig. 6 (c)) it seems that amorphous products are formed during auto combustion, but at the highest available magnification it is possible to recognize, that there are agglomerated nanoparticles with a size less than 50 nm (Fig. 6 (d)).

XRD patterns of Ni-Zn ferrite auto combustion products (Fig. 7); besides, spinel phase shows diffraction maximum of impurity phases – after the reaction forms a multiphase mixture. In case of NiFe₂O₄ ($x=0$) the peaks of the impurity phases, corresponding to hematite (Fe₂O₃) and awaruite (FeNi₃), are observed. For Ni-Zn ferrites ($0 < x < 1$) there are Fe₂O₃, FeNi₃ and zincite

(ZnO), but in case of $\text{ZnFe}_2\text{O}_4(x=1)$ only spinel and zincite are observed. Corresponding phases for different compounds can be well understood.

XRD patterns of Ni-Zn ferrite samples annealed at 700 °C (Fig. 8), show monophasic cubic spinel structure. The sharp diffraction peaks indicate a high degree of crystallization. No peaks from other phases were detected, thus indicating high purity of the synthesized products.

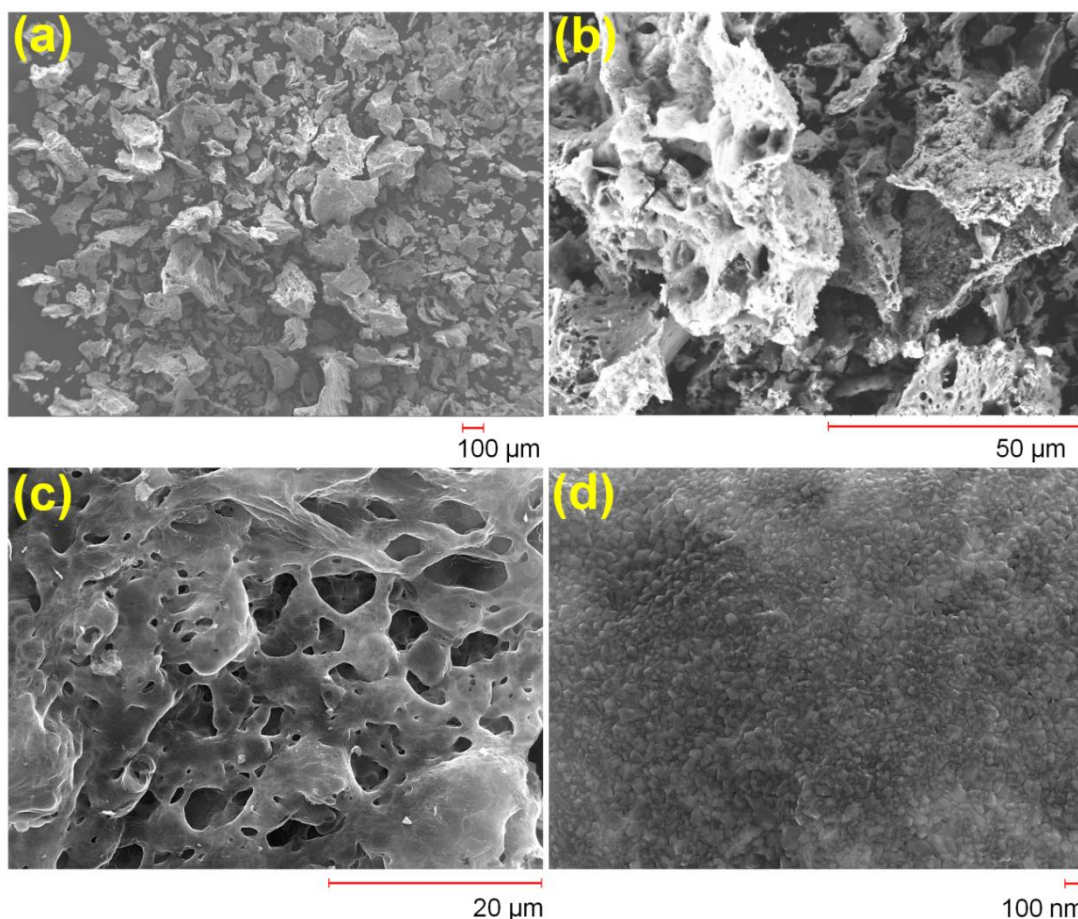


Fig. 6. SEM microphotographs of $\text{Ni}_{0.5}\text{Zn}_{0.5}\text{Fe}_2\text{O}_4$ auto combustion reaction products at different magnifications

The lattice constant a (Table 2) increases with the concentration of Zn^{2+} attributed to the smaller Ni^{2+} cations being replaced by larger Zn^{2+} cations, as well as addition of larger Zn^{2+} (0.83 Å) cause migration of smaller Fe^{3+} (0.67 Å) ions from tetrahedral sites to octahedral sites. The Zn^{2+} ions being larger than Fe^{3+} ions expand the tetrahedral sites leading to an increase of the lattice parameter [1]. The X-Ray density decreases with the increase of zinc content due to the increase of the lattice constant (Table 2).

Table 2

Structural parameters of $\text{Ni}_{1-x}\text{Zn}_x\text{Fe}_{2+z}\text{O}_{4-\delta}$ (x – Zn^{2+} content, a – lattice constant, ρ_x – theoretical density)

x	z=0	
	a, Å	ρ_x , g/cm ³
0	8,3219	5,403
0,3	8,3472	5,390
0,5	8,3739	5,378
0,7	8,4056	5,347
1	8,4213	5,362

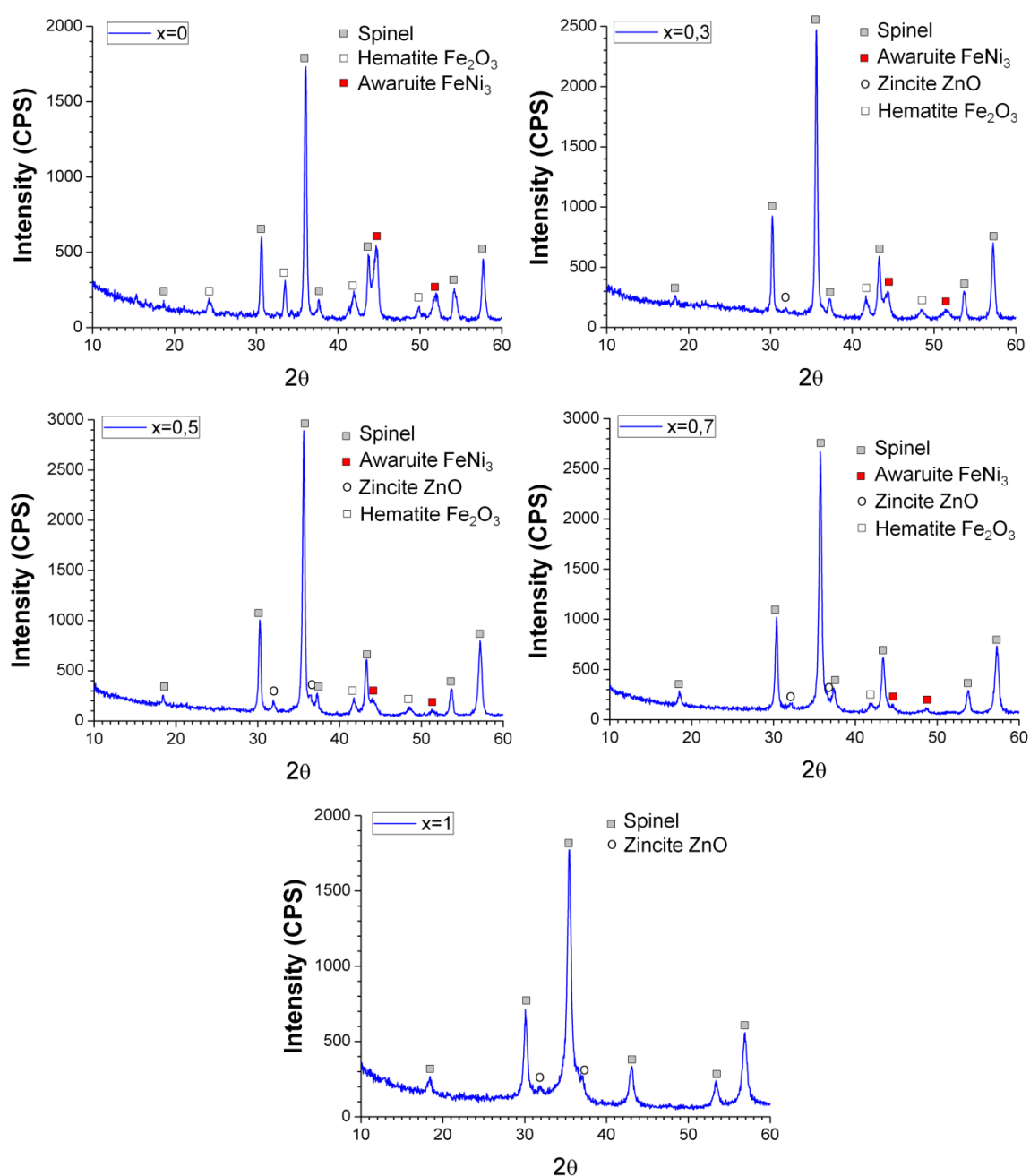


Fig. 7. XRD patterns of $\text{Ni}_{1-x}\text{Zn}_x\text{Fe}_2\text{O}_4$ after auto combustion

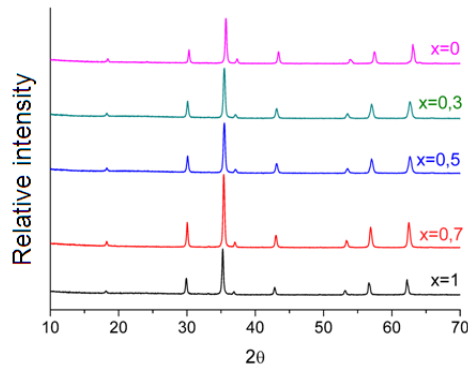


Fig. 8. XRD patterns of annealed $\text{Ni}_{1-x}\text{Zn}_x\text{Fe}_2\text{O}_4$ powders at 700°C

The influence of the composition and stoichiometry on the electric properties of Ni-Zn ferrites was measured on tablet shaped samples, which were pressed from auto combustion reaction products and sintered at 800°C . This was the minimal temperature to obtain samples with sufficient mechanical strength.

The SEM microphotographs of the fractured surfaces of the samples sintered at 800°C are shown in Fig. 9. As we can see, samples are formed from individual particles with a size ~ 100 nm. No morphological differences were apparent between samples of various compositions.

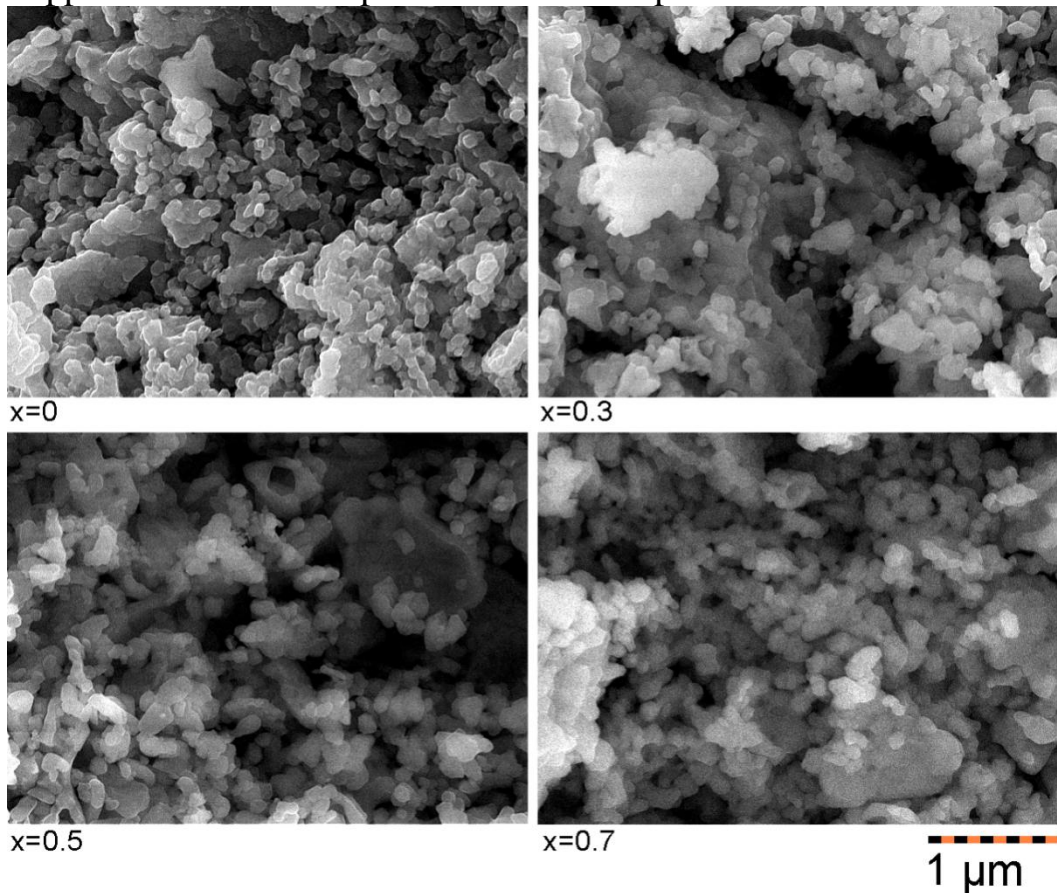


Fig. 9. SEM micrographs of $\text{Ni}_{1-x}\text{Zn}_x\text{Fe}_2\text{O}_4$ samples sintered at 800°C

The influence of zinc ion content and iron ion stoichiometry on the resistivity is shown in Fig. 10. For stoichiometric compositions ($z=0$) resistivity increases with increasing zinc content. It can be explained by relatively small zinc loss due to low sintering temperature, thus reducing Ni^{3+} to Ni^{2+} and decreasing charge carrier (hole) concentration.

Resistivity dependence from Zn content of excess-iron Ni-Zn ferrites is shown in Fig. 10. The resistivity at $x=0$ and $x=0.3$ is higher compared to stoichiometric $x=0$ and $x=0.3$, which could also be attributed to electron-hole compensation. The excess of iron facilitates the formation of Fe^{2+} and, hence, the increase of the concentration of free electrons recombining with holes. This also can be understood as oxygen vacancy formation and reduction of Ni^{3+} to Ni^{2+} . In the same way, due to the increase of Fe^{2+} concentration in excess-iron Ni-Zn ferrites, the decrease of resistivity compared with stoichiometric Ni-Zn ferrites at $x=0.7$ and $x=1$, is attributed to the addition of extra electrons. At the same time, resistivity of $x=0.7$ with an excess-iron do not decreases so much as observed by other authors who used higher sintering temperatures [2].

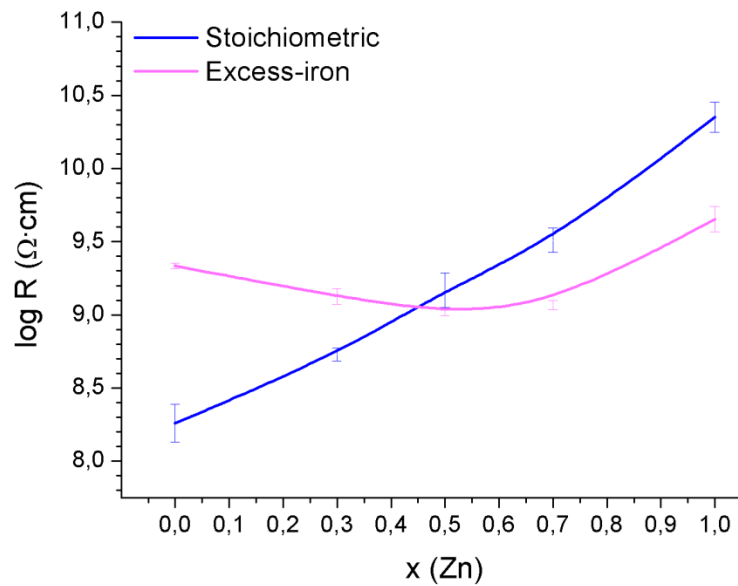


Fig. 10. DC resistivity of stoichiometric and excess-iron Ni-Zn ferrite samples

The influence of cooling rate on NiFe_2O_4 and non-stoichiometric $\text{Ni}_{1-x}\text{Zn}_x\text{Fe}_{2.1}\text{O}_{4-\delta}$ ferrite resistivity is shown in Fig. 11 (a) and (b). Resistivity of NiFe_2O_4 increases with increasing cooling time, because there is more time for Ni^{3+} reduction to Ni^{2+} or the formation of compounds with lower point defect (cation vacancy) concentration. In the same manner, with decreasing cooling rate decreases the defect (oxygen vacancy) concentration of excess iron Ni-Zn ferrites.

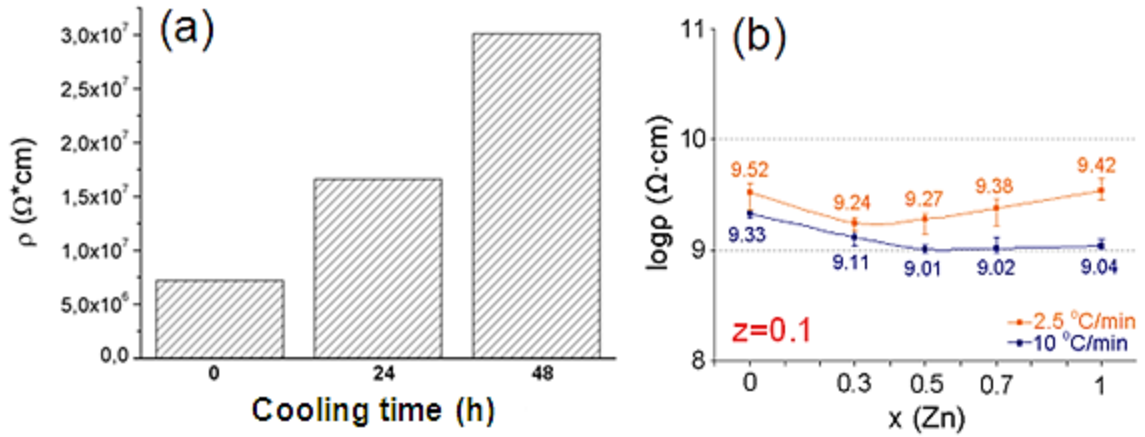


Fig. 11. Cooling time influence on (a) NiFe_2O_4 and (b) non-stoichiometric $\text{Ni}_{1-x}\text{Zn}_x\text{Fe}_{2.1}\text{O}_{4-\delta}$ ferrite electric properties

To modify electric properties, samples were additionally annealed in the vacuum for 1 hour at 800°C . During vacuum annealing the samples formed oxygen vacancies and the transition metal ions were reduced from Me^{2+} to Me^{3+} . In Fig. 12 it can be seen that resistivity of NiFe_2O_4 and ZnFe_2O_4 rapidly decreases. For example, resistivity of ZnFe_2O_4 decreases for seven orders. Also, it can be seen that resistivity of NiFe_2O_4 annealed in the air has lower, but after annealing in vacuum – higher resistivity in comparison with ZnFe_2O_4 . In case of NiFe_2O_4 , first Ni^{3+} reduces to Ni^{2+} and then Fe^{3+} to Fe^{2+} , but for ZnFe_2O_4 reduction of Fe^{3+} to Fe^{2+} starts already at the beginning of the vacuum annealing process. In case of ZnFe_2O_4 , loss of zinc ion is possible besides oxygen vacancy formation, while for NiFe_2O_4 there is only a loss of oxygen.

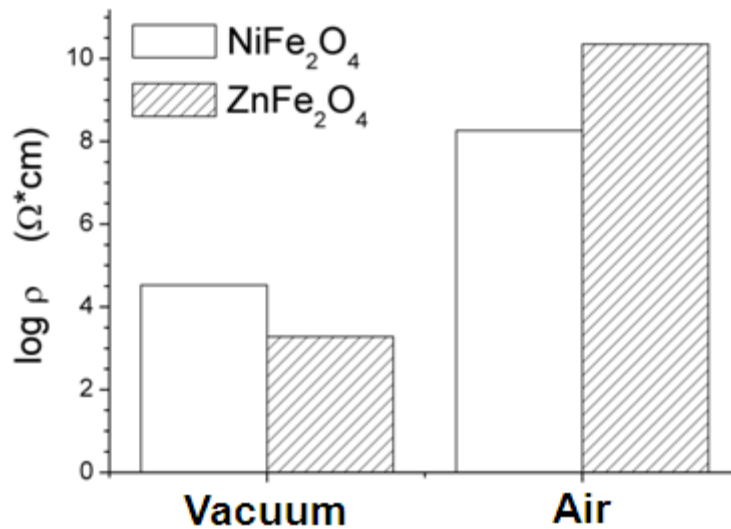


Fig. 12. Resistivity of NiFe_2O_4 and ZnFe_2O_4 annealed in vacuum and air

The temperature-dependent variation of DC resistivity is shown in Fig. 13. Resistance decreases with increasing temperature, thus demonstrating semiconducting properties of spinel type ferrites. At the same time, the

anomalous change of resistance in two temperature regions, i.e., $\sim 100^\circ\text{C}$ and $\sim 300^\circ\text{C}$ is observed. This is attributed to dehydroxylation at the lower temperature [3] and O_2 chemisorption at the higher temperature [4].

At room temperature, during formation of $-\text{OH}$ groups on the sample surface (hydroxylation), an electron is trapped in accordance with the reactions $\text{H}_2\text{O}_{\text{ads}} + \text{O}_\text{O}^x \rightarrow 2\text{OH}$ and $\text{OH} + e' \rightarrow \text{OH}'$, thus increasing the resistance of n-type and decreasing of p-type semiconductor. In reverse process (dehydroxylation) at $\sim 100^\circ\text{C}$, an electron is released back to the material.

At higher temperature ($\sim 300^\circ\text{C}$), due to oxygen chemisorption, an electron is trapped from the structure in accordance with equation $\text{O}_2 + e^- \leftrightarrow \text{O}_2^-$ [4]. This increases resistance of n-type and decreases resistance of p-type material. From Fig. 13 it can be seen that stoichiometric Ni-Zn ferrites with $x \leq 0.7$ exhibit p-type conductivity, but ZnFe_2O_4 and non-stoichiometric Ni-Zn ferrites – n-type conductivity.

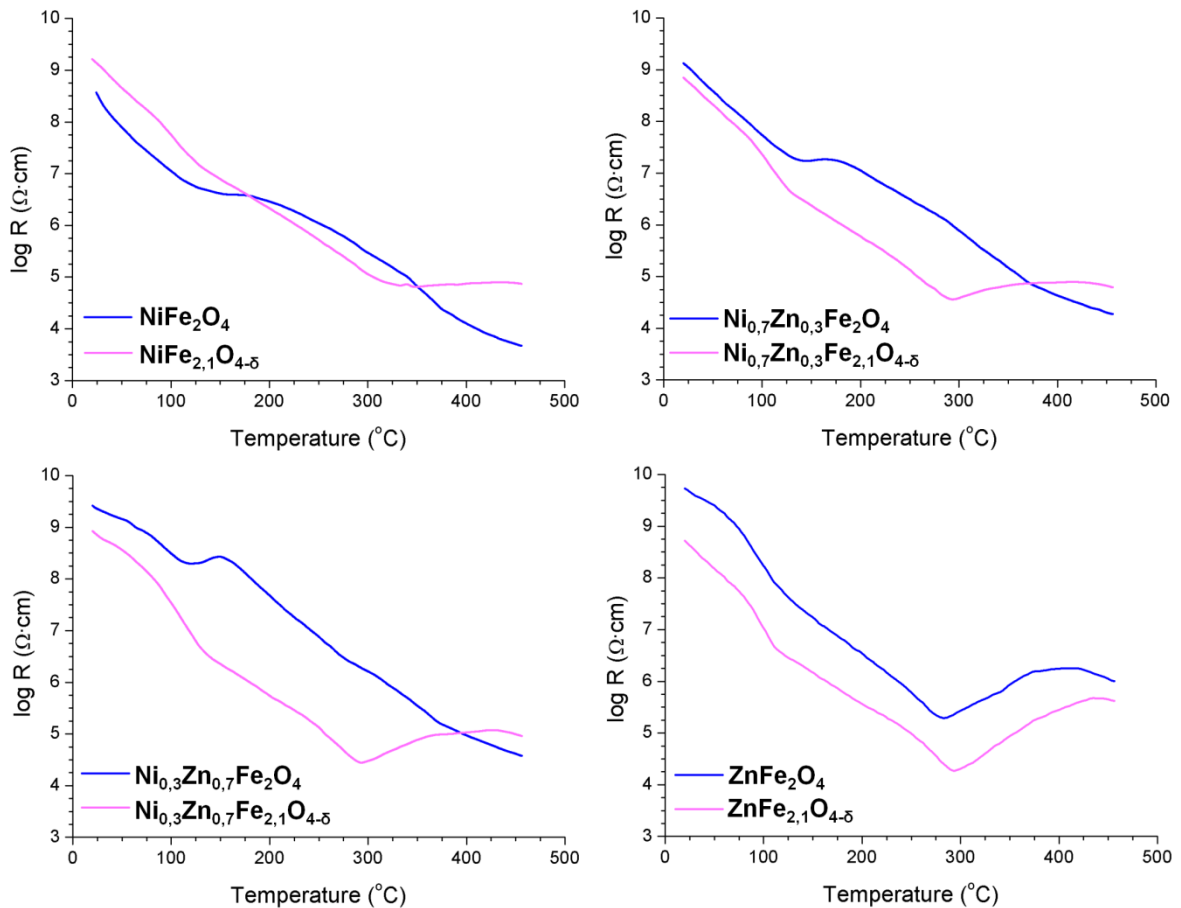


Fig. 13. DC resistivity as a function of temperature in stoichiometric and excess-iron ferrite samples

Such anomalous behaviour is due to a large specific surface area of nanostructured Ni-Zn ferrite and cannot be observed in micro-structured materials. Of course, adsorption-desorption processes occur also on the

surface of microstructured oxides, but their surface area occupies only a small part of the grain volume; thus, the influence of mentioned processes on electric resistance cannot be detected.

The change of dielectric constant ϵ and dielectric loss $\tan\delta$ with AC frequency, composition and stoichiometry is shown in Fig. 14. The ϵ and $\tan\delta$ decreases with increasing frequency due to the fact that beyond certain frequency the hopping of charge carriers can not follow the alternating field, thus decreasing polarization [5]. The dielectric constant also decreases with increasing the zinc content for stoichiometric Ni-Zn compositions, as well as for iron-excess compositions with low zinc content. This arises from a lower concentration of charge carrier and the formation of a more homogeneous electronic structure decreasing polarization. The results correlate with DC resistivity measurements, i.e. the samples of lower resistivity have a lower dielectric constant.

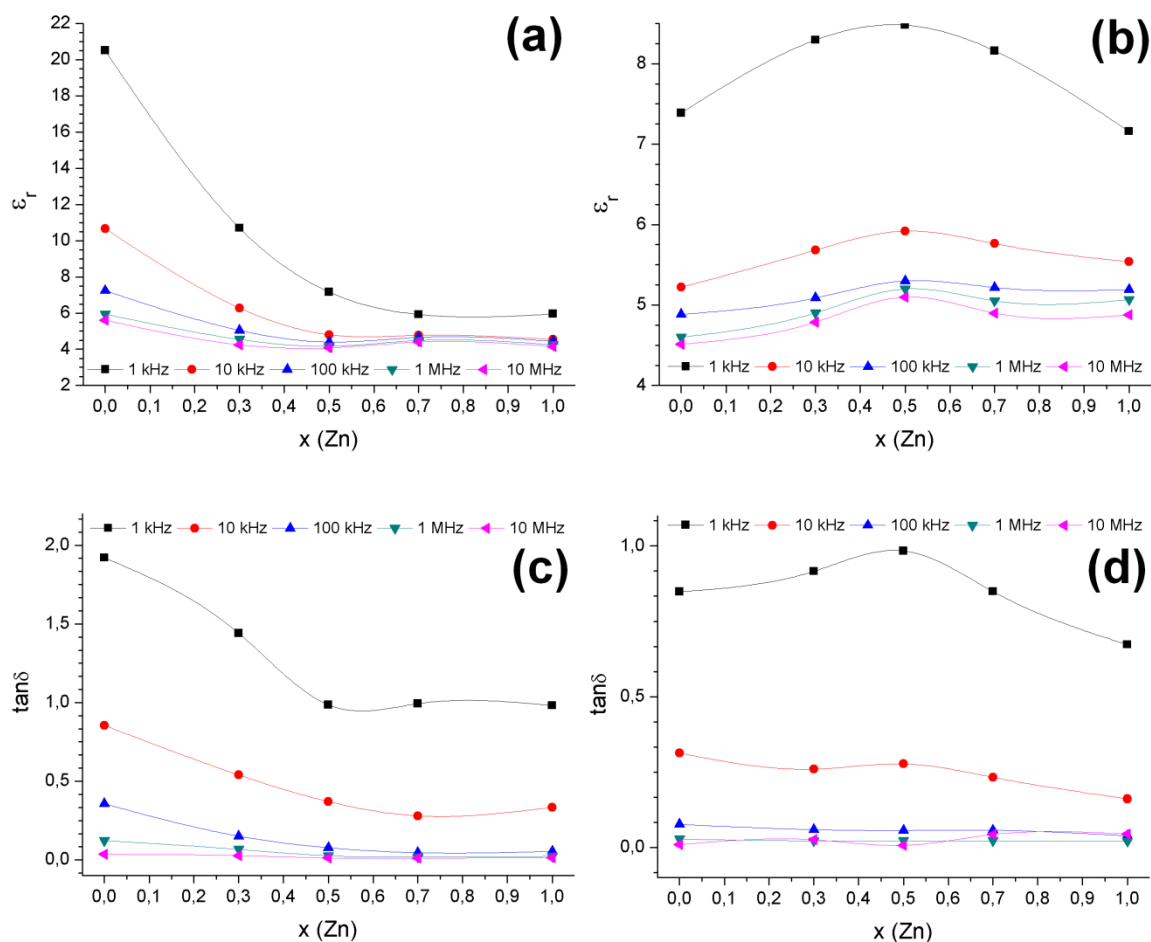


Fig. 14. The effect of AC frequency, composition and stoichiometry on Ni-Zn ferrite dielectric constant ϵ and dielectric loss $\tan\delta$ for stoichiometric ((a) and (b)), non-stoichiometric Ni-Zn ferrites ((c) and (d))

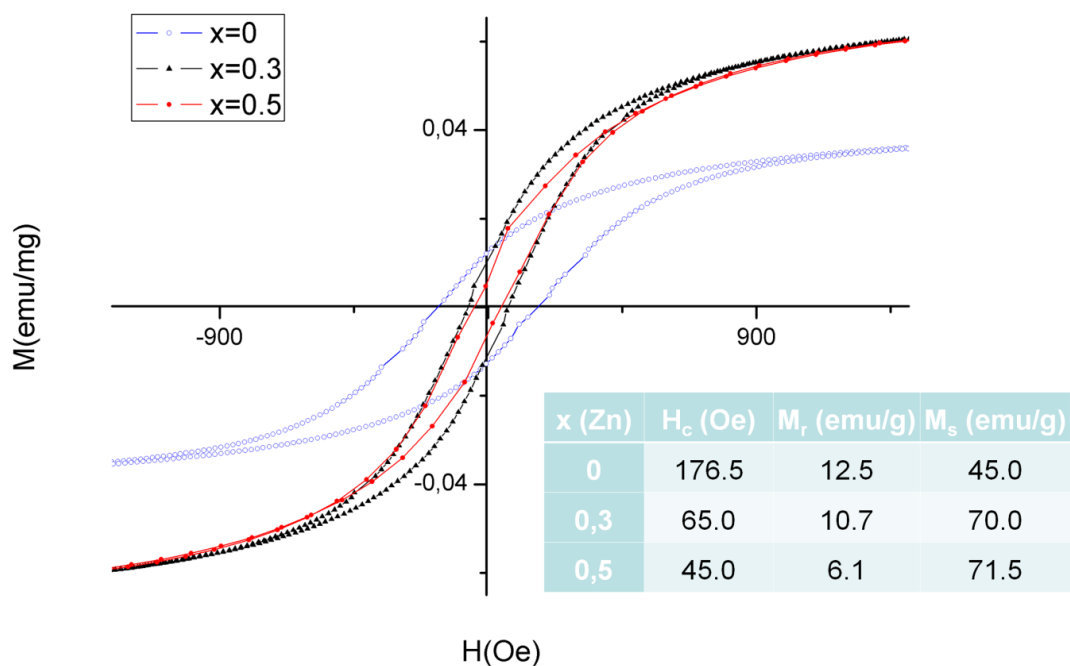


Fig. 15. Magnetic hysteresis loops and properties of $\text{Ni}_{1-x}\text{Zn}_x\text{Fe}_2\text{O}_4$ at 300 K

Magnetic hysteresis loops and properties of $\text{Ni}_{1-x}\text{Zn}_x\text{Fe}_2\text{O}_4$ at 300 K are shown in Fig. 15. With increasing zinc ion content the coercive force and remanent magnetization decreases, while the saturation magnetization increases. The obtained relationship is attributed to Fe^{3+} transition from tetrahedral to octahedral site with zinc ion addition, thus decreasing magnetic moment of tetrahedral site and increasing magnetic moment of octahedral site, as well as weakening of the tetrahedral-O-octahedral interaction [6]. During the study the magnetic properties of ZnFe_2O_4 were also measured. As expected at room temperature zinc ferrite exhibited paramagnetic properties.

For the investigation of annealing temperature influence on Ni-Zn ferrite electrical properties, auto combustion reaction powders were pressed and sintered at temperatures from 900°C to 1300°C with a step 100°C . Structural, electric and dielectric properties of the obtained samples were investigated.

XRD results confirmed that there is no change in phase purity by performing annealing at an elevated temperature (not shown here).

By using quantitative chemical analysis the divalent iron ion content concentration was measured in $\text{Ni}_{0.3}\text{Zn}_{0.7}\text{Fe}_2\text{O}_4$ sintered at different temperatures (Fig. 16). Ferrous ion concentration increases with increasing sintering temperature attributed to the increase of Zn^{2+} loss [1]. The obtained results are comparable with the results obtained by other authors [7].

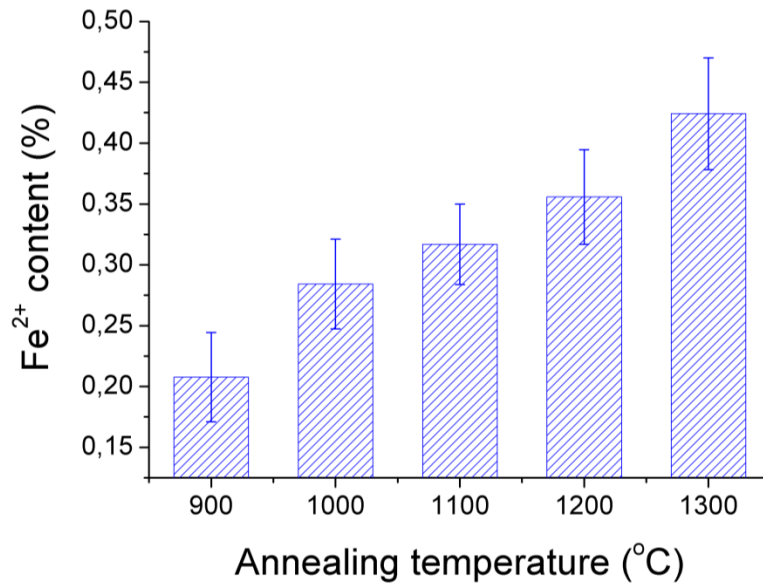


Fig. 16. Sintering temperature influence on Fe²⁺ content in Ni_{0.3}Zn_{0.7}Fe₂O_{4-δ}

The SEM micrographs of Ni_{0.3}Zn_{0.7}Fe_{2.1}O_{4-δ} sintered at different temperatures are shown in Fig. 17. Grain size increases and porosity decreases with increasing temperature attributed to the intensification of sintering and diffusion processes. Samples sintered at 900°C show the presence of nanosized grains. The sintering of powders has produced a grain size of about 0.08 μm to 2.5 μm by changing sintering temperature from 900 °C to 1300°C.

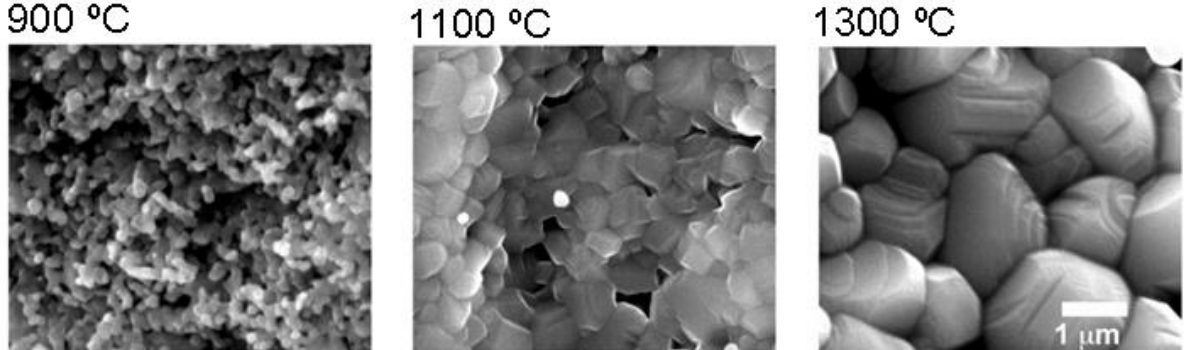


Fig. 17. SEM images of the fracture surface of Ni_{0.3}Zn_{0.7}Fe_{2.1}O_{4-δ} sintered at different temperatures (1 μm bar on the last micrograph refers to all images)

Electrical resistivity, porosity and grain size dependence on sintering temperature for stoichiometric Ni-Zn ferrites are shown in Fig. 18. For all compositions with $x > 0.3$ resistivity decreases with increasing temperature, due to the decrease of porosity, increase of Fe²⁺ content and grain size. The larger grain size provides less grain boundaries that act as barriers to the flow of electrons [7]. It is known, that grain boundaries for n-type transition metal oxide semiconductors have higher resistivity than a bulk. This is due to the fact that in grain boundary there is faster oxidation of Fe²⁺ to Fe³⁺, for example [8].

Ni-Zn ferrites with higher zinc ion content show greater decrease of resistivity with sintering temperature which is attributed to a greater loss of zinc ion from the material, which favours the formation of Fe^{2+} .

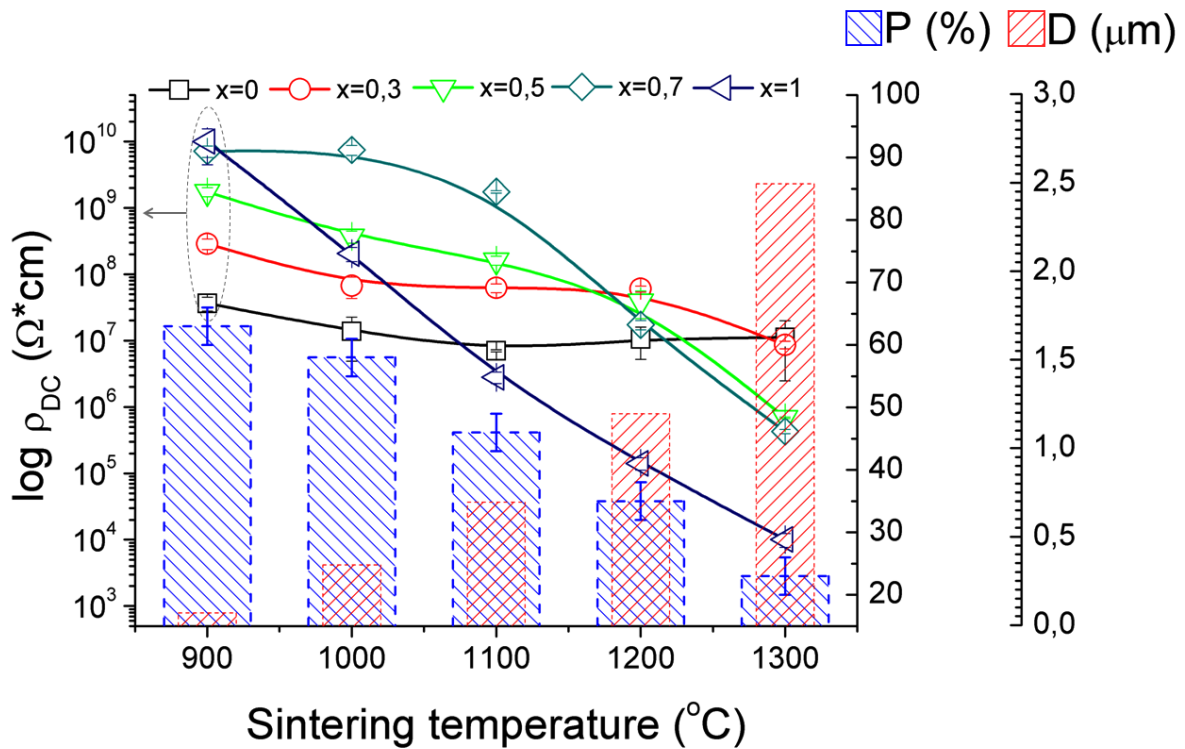


Fig. 18. Electrical resistivity, porosity and grain size dependence on sintering temperature for stoichiometric Ni-Zn ferrites

It is noteworthy that resistivity of $\text{Ni}_{1-x}\text{Zn}_x\text{Fe}_2\text{O}_4$ ferrites with $x=0$ and $x=0.3$ almost does not change with sintering temperature. This is due to the formation of Me^{2+} vacancies or dominance of p-type conductivity. It is known that for p-type transition metal oxide semiconductors grain boundary has lower resistance in comparison with a bulk. The charge transfer occurs in the outer shell of the grain; thus, its size does not influence the electrical resistivity.

The electrical properties of various phases (boundary and bulk of the grain) presented in the material could be determined by the use of impedance spectroscopy (IS). The complex impedance spectra of polycrystalline material consisting of grains, in which the resistance of the outer shell differs from that of the bulk, will result in series of two connected arcs (Fig. 19 (a)). Experimentally obtained grain and grain boundary resistance of $\text{Ni}_{0.3}\text{Zn}_{0.7}\text{Fe}_{2.1}\text{O}_{4-\delta}$, sintered at different temperatures, and is shown in Fig. 19 (b). The resistance of the grain boundary (R_V) are found to be higher than the resistance of the grain (R_T), as well as both R_V and R_T decreases by increasing annealing temperature. The higher resistance of the grain boundary is due to the fact that at the outer shell of the grain there is faster oxidation of Fe^{2+} to

Fe^{3+} , thus decreasing the charge carrier (electron) or oxygen vacancy concentration.

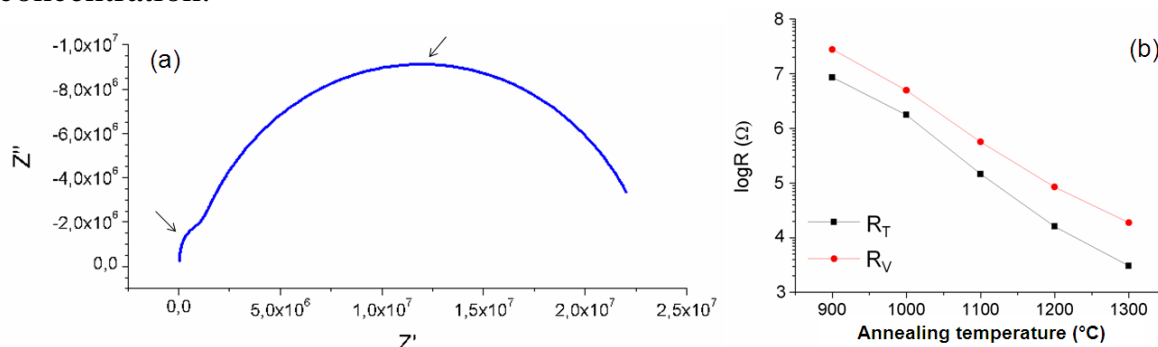


Fig. 19. (a) Complex impedance spectra for $\text{Ni}_{0.3}\text{Zn}_{0.7}\text{Fe}_{2.1}\text{O}_{4-\delta}$ sintered at 900°C and (b) grain boundary (R_V) and volume (R_T) resistance for $\text{Ni}_{0.3}\text{Zn}_{0.7}\text{Fe}_{2.1}\text{O}_{4-\delta}$ sintered at different temperatures

Spinel ferrites for high-frequency applications have been used for several decades, yet due to the optimization of size, weight, power consumption and performance of electrical devices (for example, mobile phones, laptops), the ferrite thin films (thickness $< 1\mu\text{m}$) are required. At the same time, information about ferrite thin films is not widely available and all advantages of the ferrite thin films can hardly be found. Due to this reason, by using spray pyrolysis, $\text{Ni}_{1-x}\text{Zn}_x\text{Fe}_2\text{O}_4$ thin films were obtained and characterized.

XRD analysis (Fig. 20 (a)) confirmed the formation of $\text{Ni}_{1-x}\text{Zn}_x\text{Fe}_2\text{O}_4$ spinel ferrites. Only spinel phase characteristic peaks were observed. The uplift between the peaks corresponding to crystallographic planes (111) and (311) is due to the X-Ray diffraction from amorphous glass substrate. The lattice constant of Ni-Zn ferrite thin films (Fig. 20 (b)) increases with the concentration of Zn^{2+} in the same manner as ferrite powders.

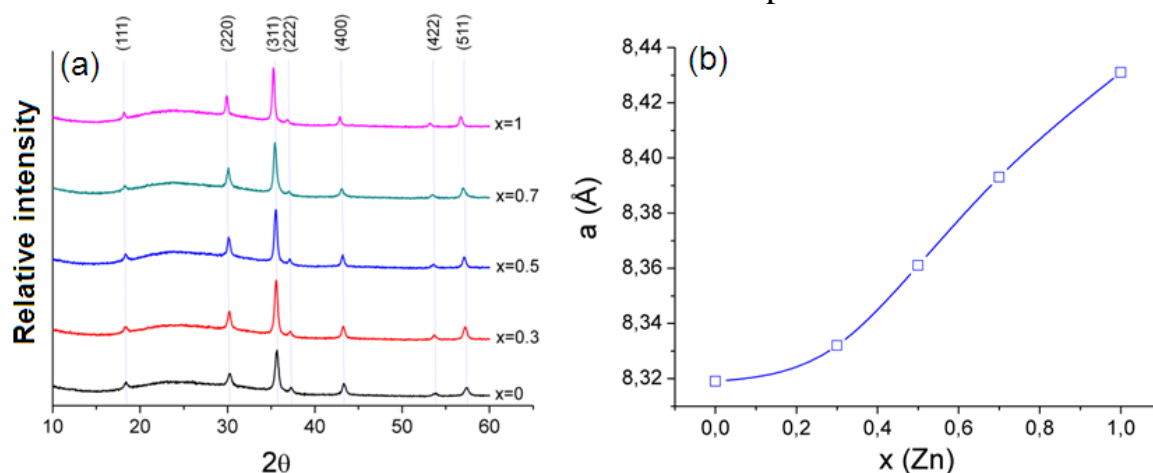


Fig. 20. (a) XRD patterns of $\text{Ni}_{1-x}\text{Zn}_x\text{Fe}_2\text{O}_4$ thin films and (b) lattice constant a dependence from Zn^{2+} content

Cross-section of the ZnFe_2O_4 thin film is shown in Fig. 21. Overall, thicknesses of the thin films were ~ 500 nm. Also, the SEM micrograph (Fig.

21) reveals quite homogeneous fixed layer with a flat surface. Film structure is formed from densely packed spherical nanosized grains.

Properties of the Ni-Zn ferrite thin films are shown in Table 3. DC resistivity of Ni-Zn ferrite films increases by increasing zinc content. In the Ni-Zn ferrite films due to a low processing temperature (500°C), the loss of zinc is comparatively negligible, thus the resistivity increases. The obtained change manner of resistivity correlates to that of Ni-Zn ferrites sintered at 800°C. At the same time, in spite of dense microstructure of the thin film, resistivity is very high. From the practical point of view, it is important to obtain dense Ni-Zn ferrites with high resistivity, because presence of pores in the structure decreases magnetic susceptibility.

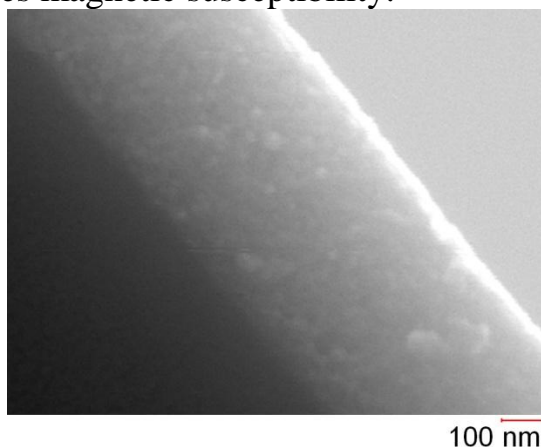


Fig. 21. Cross-section of $ZnFe_2O_4$ thin film obtained by spray pyrolysis

The observed $\tan\delta$ values correlate with resistivity measurements. Samples with lower resistivity possess smaller local polarization and lower $\tan\delta$ due to lower concentration of charge carriers. The observed dielectric losses are lower than nanosized Ni-Zn ferrite powder samples at 100 kHz [9] attributed to lower defect concentration and the difference between resistance of grain and grain boundary, which arises from Maxwell-Wagner interfacial type of polarization. At the same time, dielectric losses are comparable with planar Ni-Zn ferrite inductors obtained by more complex electrophoresis ferrite deposition [10].

Table 3

Properties of $Ni_{1-x}Zn_xFe_2O_4$ thin films: D_k – thickness, R_A – average roughness, d_0 – crystallite size, a – lattice constant, E_g – direct band gap energy, ρ_x - theoretical density, ρ – electrical resistivity, $\tan\delta$ – dielectric loss

x	D_k , nm	R_A , nm	d_0 , nm	a, Å	E_g , eV	ρ_x , g/cm ³	ρ , Ω·cm	$\tan\delta$ (100 kHz)
0	~400	61 ± 2	18,8	8,319	1,90	5,41	4,12·10 ⁶	0,024
0.3	~600	67 ± 2	22,5	8,332	2,10	5,42	1,22·10 ⁷	0,020
0.5	~500	36 ± 2	23,3	8,361	2,30	5,40	2,66·10 ⁸	0,019
0.7	~550	44 ± 2	22,9	8,393	2,52	5,37	1,04·10 ⁹	0,015
1	~500	35 ± 2	29,0	8,431	2,70	5,34	1,82·10 ¹⁰	0,011

Gas sensitivity of metal oxide semiconductors is directly connected with their electric properties. As we saw previously, electrical properties of Ni-Zn ferrites can be varied in wide orders; thus, attention is paid also to the investigation of Ni-Zn ferrite gas sensing properties. The gas sensing measurements are also useful for better understanding of electric properties of transition metal oxides.

Within the study, zinc ion and cooling condition influence on NiFe₂O₄ and iron ion stoichiometry influence on Ni-, Ni-Zn and Zn- ferrite gas response were investigated. Gas sensitivity was also measured for ZnFe₂O₄ thin films.

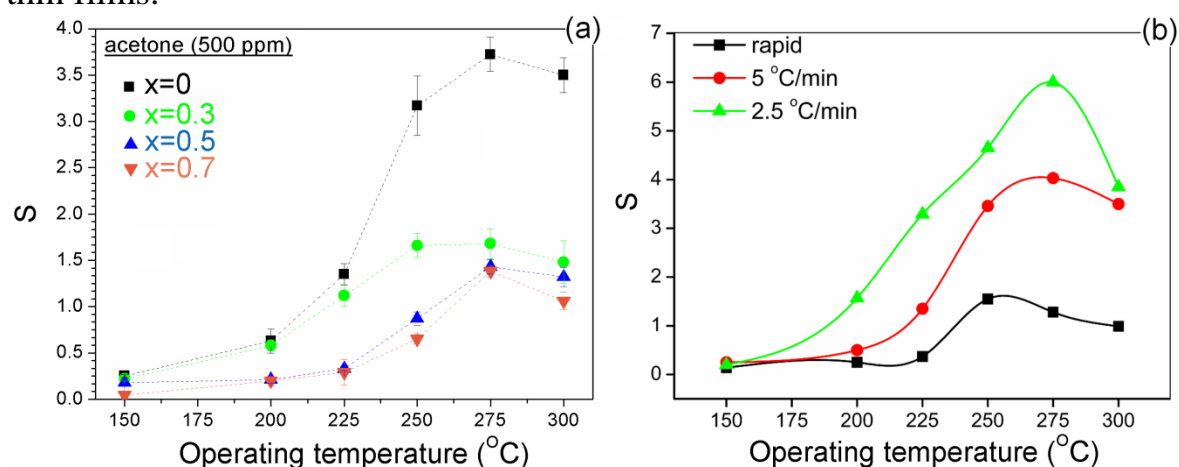


Fig. 22. Temperature, composition (a) and cooling rate (b) influence on the response (S) of Ni_{1-x}Zn_xFe₂O₄ to acetone (500ppm)

Response to gas for NiFe₂O₄ decreases with increasing zinc ion content (Fig. 22 (a)), but increases with decreasing cooling rate (Fig. 22 (b)). Decrease of NiFe₂O₄ response with Zn²⁺ addition is attributed to decrease of Ni²⁺ concentration in the octahedral site, thus providing the formation of Fe²⁺. The reduction of Fe³⁺ is opposite process to Ni²⁺ oxidation; thus, it will restrict oxygen adsorption for interaction with test gas on NiFe₂O₄ grain surface and decrease gas response. Moreover, the gas interaction with chemisorbed oxygen will cause reduction of Ni³⁺ to Ni²⁺ and increase of resistivity or reduction of Fe³⁺ to Fe²⁺, and increase of conductivity of the spinel type ferrite, thus giving lower total change of the resistance. A schematic representation of the idea is shown in Fig. 23.

The increase of NiFe₂O₄ sensitivity with decreasing cooling rate after annealing is attributed to lower cation vacancy concentration or higher Ni²⁺ content. As it was concluded from the resistivity measurements, rapidly cooled samples are characteristic with higher Ni³⁺ content. Trivalent nickel ion is not able to attract active oxygen for the interaction with a test gas, because in spinel structure Ni³⁺ cannot occupy higher oxidation state.

With iron ion stoichiometry it is possible to change the type of conductivity of spinel ferrite (Fig. 24) or increase gas response to a test gas

(Fig. 25). The addition of iron ion creates oxygen vacancies and due to the charge imbalance reduces trivalent iron or nickel ions to divalent in accordance with the equation: $2xFe_{Fe}^{3\bullet} \rightarrow 2xFe_{Fe} + 3xV_o^{2\bullet} + 6Me'_{Me}$.

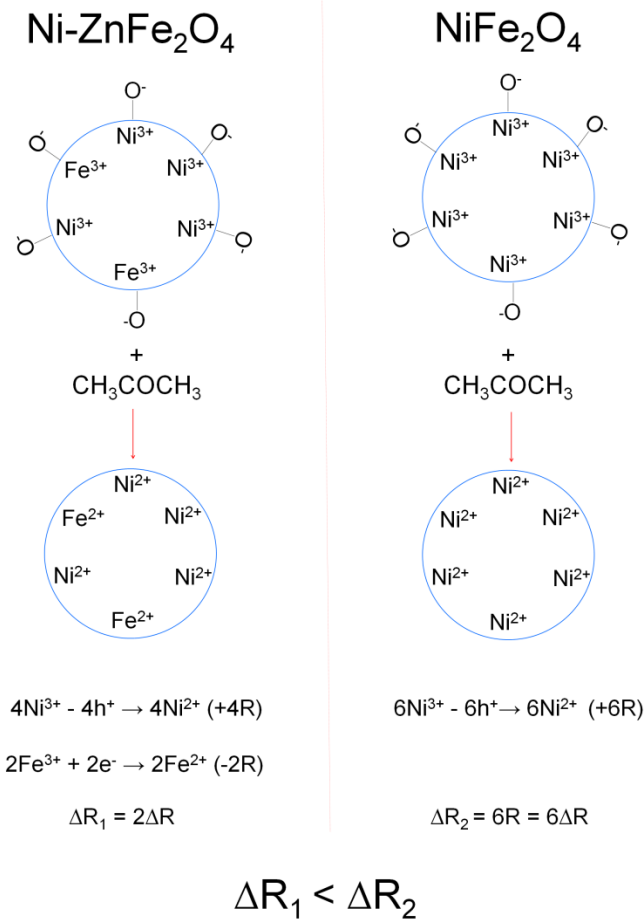


Fig. 23. Schematic representation of gas sensing mechanism for Ni-Zn ferrites

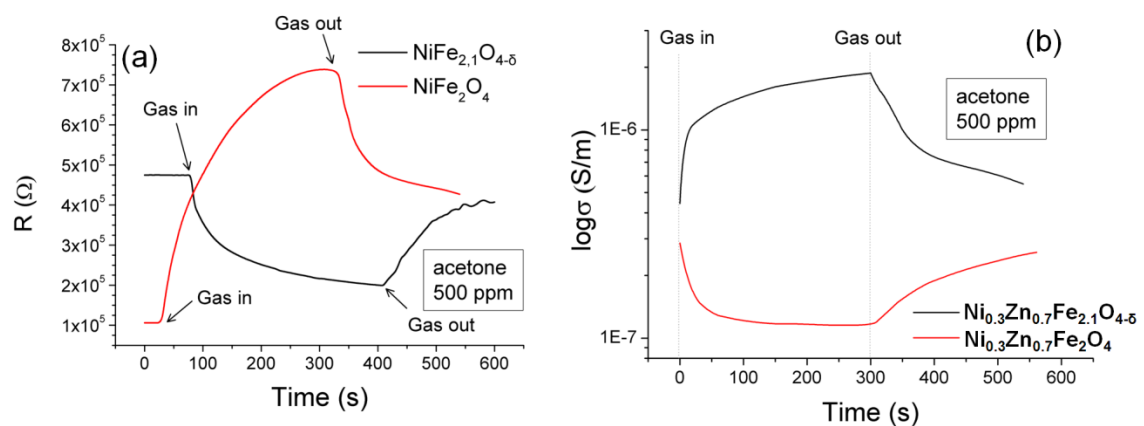


Fig. 24. Response-recovery behaviour to acetone (500 ppm) at 275 °C for stoichiometric and excess-iron ferrite (a) NiFe₂O₄, (b) Ni_{0.3}Zn_{0.7}Fe_{2.1}O_{4.5}

As we can see in Fig. 24, with iron-excess semiconductor nature of NiFe₂O₄ ferrite changes from p-type to n-type, because the resistance of

stoichiometric NiFe_2O_4 increases with acetone introduction, but for excess-iron – decreases. This is due to the fact that for iron-excess compositions all Ni^{3+} and part of the Fe^{3+} ions are reduced to Ni^{2+} and Fe^{2+} , respectively.

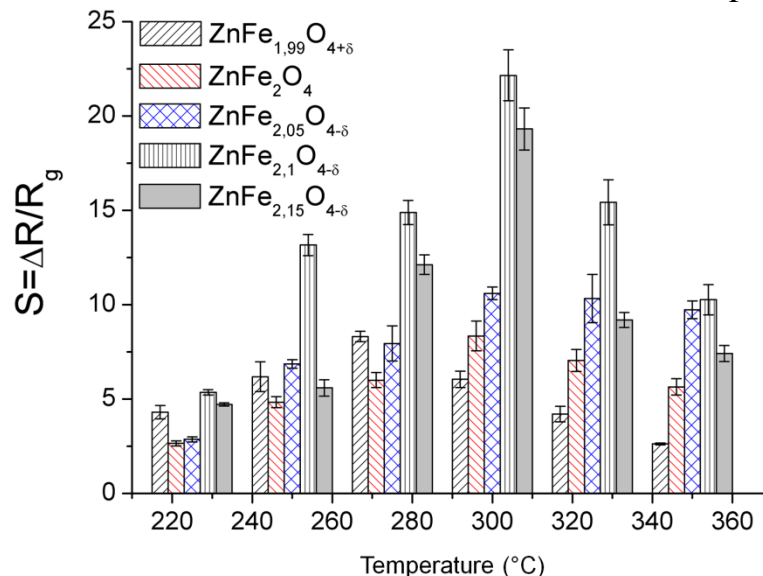


Fig. 25. The influence of iron ion stoichiometry on $\text{ZnFe}_{2\pm z}\text{O}_{4\pm\delta}$ gas response to ethanol (500 ppm)

Iron ion stoichiometry in zinc ferrite was varied in wide orders ($\text{ZnFe}_{2+z}\text{O}_{4-\delta}$, where $z = 0; 0.05; 0.1$ and 0.15) and gas response of the obtained compositions was measured. As we can see in Fig. 25 iron-excess zinc ferrites exhibit much higher gas response. Sensitivity increases by going from iron deficient to excess. The increase of gas response can be explained by Fe^{2+} or oxygen vacancy formation. This promotes oxygen chemisorption for the interaction with a test gas. By reaching $z > 0.1$, sensitivity drops again. The decrease of gas response, if $z > 0.1$, is attributed to remarkable decrease of depletion layer width shown by the impedance spectroscopy. By fitting equivalent circuit to complex impedance spectra measured in the air and 500 ppm ethanol atmosphere, it was possible to estimate the resistance and response of the bulk and grain boundary. In Fig. 26 we can see that ratio between depletion layer (S_d) and the bulk response (S_b) increases with excess-iron attributed to decrease of depletion layer width. $\text{ZnFe}_{2.15}\text{O}_{4-\delta}$ exhibits much higher ratio between signals. It is known that the adsorption of oxygen on an n-type semiconductor particle surface produces electron-depleted space-charge layer. With an increase of charge carrier concentration in the n-type material, the depletion layer width and gas sensitivity decreases.

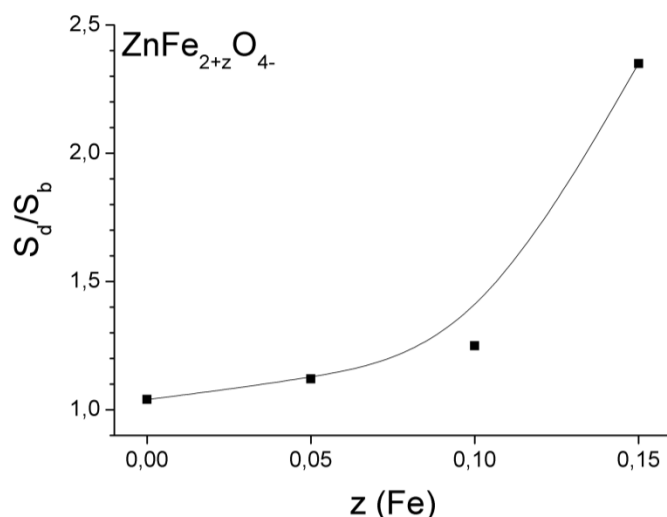


Fig. 26. Iron ion stoichiometry influence on ratio between depletion layer (S_d) and bulk response (S_b) to 500 ppm ethanol at 300°C for $ZnFe_2O_4$

It was observed for all compositions that with an increasing operating temperature the sensitivity increases to maximum and then decreases. The presented sensor tendency is attributed to the increase of concentration of oxygen species on the surface by replacing adsorbed hydroxyl groups and conversion of adsorbed oxygen species by following reactions: $O_{2(gas)} \rightarrow O_{2(ads)} \rightarrow O_{2(ads)}^- \rightarrow 2O_{(ads)}^- \rightarrow 2O_{(ads)}^{2-}$, thus attracting more electrons from a semiconductor [3]. The decrease of sensitivity after maximum can be attributed to the reduction of oxygen adsorption ability at higher temperatures.

For all sample groups also the microstructure was studied. It was found, that composition, stoichiometry and cooling rate do not leave influence on grain size and porosity. Also, selectivity was measured. It was found that samples show low selectivity over tested gases and the sensing response for all compositions falls into the order: ethanol>acetone>isopropanol>xylene>toluene>heptane>benzene. By studying response-recovery behaviour, it was found that the time taken to reach 90% of the maximum ΔR is ~ 2 minutes. The recovery time for the tested samples does not reach 90% from ΔR even after 5 minutes. The long response and recovery time could be attributed to the bulk nature of the sensor element.

Grain size influence on gas sensitivity was measured for $Ni_{0,3}Zn_{0,7}Fe_{2,1}O_{4-\delta}$. To obtain different grain sizes, samples were sintered in temperatures from 900 to 1300°C. Gas response decreases with increasing sintering temperature due to the increase of grain size. It is known that with increasing grain size decreases specific surface area for oxygen adsorption.

To increase the response-recovery time and sensitivity, a thin film of $ZnFe_2O_4$ was deposited on commercial sensor platform (see Fig. 4) by using spray pyrolysis. The SEM micrograph and XRD pattern of the sensor film is shown in Fig. 27 (a) and (b), respectively.

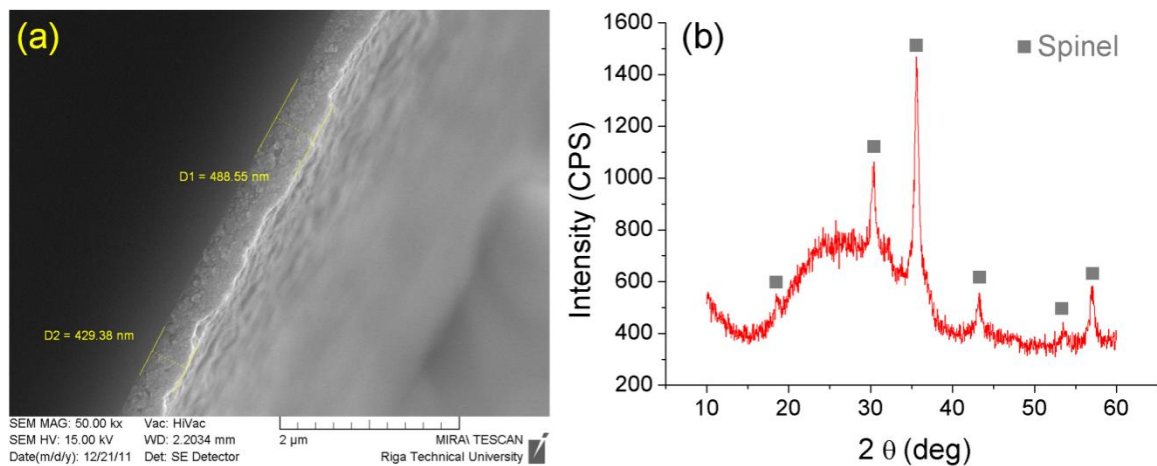


Fig. 27. ZnFe₂O₄ thin film gas sensor SEM microphotography (a) and XRD pattern (b)

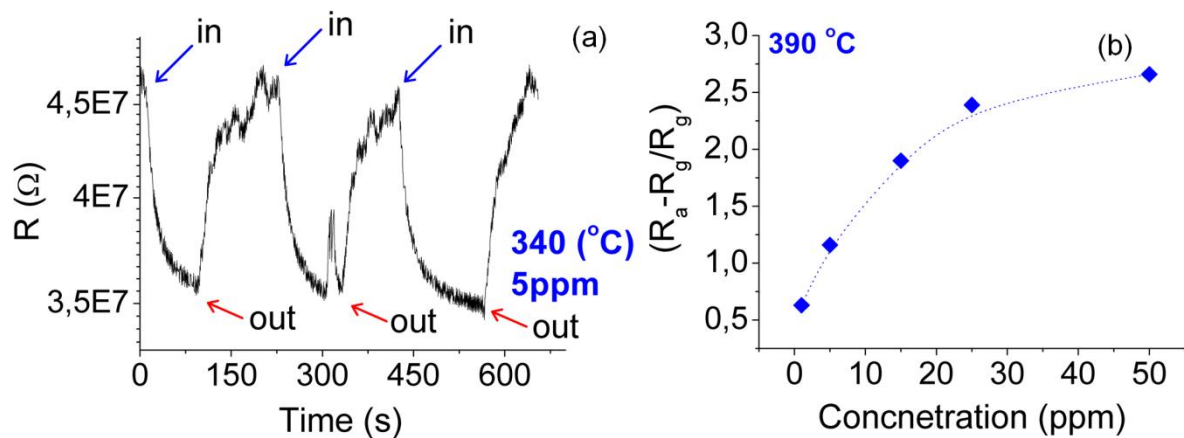


Fig. 28. (a) Response-recovery behaviour of ZnFe₂O₄ thin film gas sensor to 5 ppm ethanol (b) response dependence from gas concentration

The response-recovery behaviour of ZnFe₂O₄ thin film gas sensor to 5 ppm ethanol is shown in Fig. 28 (a). As expected, the sensor material exhibits n-type conductivity, as well as fast and fully reversible response-recovery behaviour. The response time or the time to reach 90% of the maximum ΔR was less than 40s, but the recovery time was less than 120s.

The response dependence from ethanol concentration from 1 ppm to 50 ppm at an optional operating temperature (390 °C) is shown in Fig. 28 (b). It can be seen that the sensor is able to detect ethanol at a concentration lower than 1 ppm. The magnitude of the response tends to saturate at 50 ppm. For comparison, a tablet shaped gas sensors tend to saturate at 7000 ppm.

Overall conclusions

1. The Sol-gel combustion method can be used to obtain monophasic spinel type Ni-Zn ferrite nanopowders by taking annealing at temperature not lower than 700°C.
2. Electrical resistivity of nanostructured Ni-Zn ferrites, contrary to microstructured Ni-Zn ferrites, increases with increasing zinc ion content, due to its relatively low processing temperatures and an electron-hole recombination.
3. For nanostructured excess-iron $\text{Ni}_{1-x}\text{Zn}_x\text{Fe}_2\text{O}_4$ electrical resistivity increases if $x < 0.5$ due to the charge carrier concentration, but decreases if $x > 0.5$ attributed to the addition of extra Fe^{2+} .
4. The temperature-dependent variation of DC resistivity for nanostructured Ni-Zn ferrites shows the anomalous change of conductance with temperature in two temperature regions, i.e., $\sim 100^\circ\text{C}$ and $\sim 300^\circ\text{C}$. This can be attributed to the dehydroxylation at the lower temperature and O_2 chemisorption at the higher temperature. It is shown that from the resistance character it is possible to estimate the type of conductivity of the material. $\text{Ni}_{1-x}\text{Zn}_x\text{Fe}_2\text{O}_4$ ferrites with $x \leq 0.7$ provide p-type conductivity, but ZnFe_2O_4 and excess-iron Ni-Zn ferrites n-type conductivity.
5. The change of the dielectric constant and loss of the nanostructured Ni-Zn ferrites correlate with DC resistivity measurements and show that for the nanostructured samples there is lower interfacial and local polarization.
6. With increasing sintering temperature, increases also the grain size, Fe^{2+} content, yet the porosity decreases. For p-type, in comparison with n-type ferrites, resistivity almost does not change with sintering temperature due to grain boundary having lower resistance in comparison with a bulk.
7. It was shown that by using spray pyrolysis with an aqueous solution of metal nitrates, it is possible to deposit homogeneous well-crystallized monophasic nanostructured Ni-Zn ferrite films with different zinc content and thickness $\sim 500\text{nm}$. The film structure is formed from densely packed spherical nanosized ($< 50\text{nm}$) grains. The obtained change manner of the resistivity correlates with that of Ni-Zn ferrites sintered at 800°C , but at the same time, in spite of dense microstructure of the thin film, resistivity is very high.
8. Ni-Zn ferrite gas sensor sensitivity is affected by the cooling rate after annealing, composition and stoichiometry. The change of the gas response is mainly connected with the change of concentration of oxygen or cation vacancies.
9. By increasing iron content in $\text{ZnFe}_{2+z}\text{O}_{4\pm\delta}$ from $z = -0.01$ to $z = 0.1$ the material response to a test gas increases up to 3 times. For the samples with $z > 0.1$, sensitivity starts to decrease. It was observed from the

impedance spectroscopy measurements that the increase of sensitivity is attributed to the increase of conductivity or charge carrier (electron) concentration. With increasing iron ion content decreases depletion layer width; thus, sensitivity for $z > 0.1$ also decreases.

10. ZnFe₂O₄ thin film gas sensor, which is able to detect ethanol at a concentration lower than 1 ppm, was obtained.

STATEMENTS TO DEFEND

1. The DC resistivity of nanostructured Ni-Zn ferrites increases with increasing zinc ion content due to the decrease of charge carrier (hole) concentration, attributed to Ni³⁺ reduction to Ni²⁺.
2. It is possible to estimate the type of conductivity of nanostructured Ni-Zn ferrites by measuring the resistivity dependence on temperature.
3. An original method is developed and based on impedance spectroscopy to found the change of sensitivity of metal oxide gas sensors.
4. The increase of iron ion content in zinc ferrite till the defined concentration will increase its sensitivity due to the equilibrium between the concentration of charge carriers and depletion width.

REFERENCES

1. Gul I.H., Ahmed W., Maqsood A. Electrical and magnetic characterization of nanocrystalline Ni-Zn ferrite synthesis by coprecipitation route// Journal of Magnetism and Magnetic Materials – 2008. – No. 320. – pp. 270–275.
2. Van Uitert L.G. Dielectric properties of conductivity in ferrites// Proceedings of the IRE – 1956. – No. 1. – pp. 1294–1303.
3. Giber J., Perczel I.V., Gerblinger J., Lampe U., Flischer M. Coadsorption and cross sensitivity on high temperature semiconducting metal oxides: water effect on the coadsorption process// Sensors and Actuators B-Chemical – 1994. – No. 18. – 19. pp.113–118.
4. Tianshu Z., Hing P., Jiancheng Z., Lingbing K. Ethanol-sensing characteristics of cadmium ferrite prepared by chemical coprecipitation. Materials Chemistry and Physics – 1999. – No. 61 – pp.192.–198.
5. Mohan G.R., Ravinder D., Reddy A.V.R., Boyanov B.S. Dielectric properties of polycrystalline mixed Ni-Zn ferrites// Materials Letters – 1999. – No. 40. – pp. 39–45.
6. Verma A., Goel T.C., Mendiratta R.G., Kishan P. Magnetic properties of nickel-zinc ferrites prepared by the citrate precursor method// Journal of Magnetism and Magnetic Materials – 2000. – No. 208. – pp.13–19.

7. Parvatheeswara R.B., Rao K.H. Effect of sintering conditions on resistivity and dielectric properties of Ni–Zn ferrites// Journal of Materials Science – 1997. - No. 32. - pp.6049 -6054.
8. Fang C., Zhou D.X., Gong S.P. Voltage effect in PTCR ceramics: Calculation by the method of tilted energy band// Physica B – 2010. – No. 405. – pp.852- 856.
9. Atif M., Nadeemb M., Grossingera R., Turtelli S. R. Studies on the magnetic, magnetostrictive and electrical properties of sol–gel synthesized Zn doped nickel ferrite// Journal of Alloys and Compounds – 2011. – No. 509. – pp.5720–5724.
10. Lee J.J., Hong Y.K., Bae S., Park J.H., Jalli J., Abo G.S., Syslo R., Choi B.C., Donohoe G.W. High-Quality Factor Ni-Zn Ferrite Planar Inductor// IEEE Transactions on Magnetics – 2010. – No. 46. – pp.2417. – 2420.

LIST OF AUTHOR PUBLISHED PAPERS

Articles in journals and scientific proceedings

1. A. Sutka, G. Mezinskis. Characterization of sol-gel auto-combustion reaction and attained products. Material Science and Applied Chemistry. Vol. 22 (1), 2010, pp. 51-56. ISSN 1407-7353.
2. A. Sutka, G. Mezinskis, A. Pludons, I. Juhnevisa. Synthesis and Analysis of Spinel Type Ferrite Nanoparticles. Latvian Journal of Chemistry. 2010. No. 1. pp.17-25. ISSN 0868-8249.
3. A. Sutka, G. Mezinskis, A. Pludons. Preperation of dissimilar ferrite compounds by sol-gel auto-combustion method. CHEMINĒ TECHNOLOGIJA. 2010. No. 1 (54) pp. 41-46. ISSN 1392-1231.
4. A. Sutka, G. Mezinskis, A. Pludons, S. Lagzdina. Structural and electric properties of nanostructured spinels ferrites obtained by auto-combustion method. CYSENI 2010, May 27-28, Kaunas, Lithuania. ISSN 1822-7554
5. A. Sutka, G. Mezinskis, A. Pludons, S. Lagzdina. Characterization of sol-gel auto-combustion derived spinels ferrite nano-materials. Energetika, 2010, 56, pp. 254-259.
6. A. Sutka, K.A. Gross, G. Mezinskis, G. Bebris, M. Knite. The effect of heating conditions on the properties of nano- and microstructured Ni–Znferrite. Physica Scripta, 2011, 83, 025601
7. A. Sutka, G. Mezinskis, S. Lagzdina, G. Bebris. Effect of cooling conditions on nano-sized NiFe₂O₄ electrical properties. Advanced Materials Research. 2011, 222, pp. 263-266.
8. A. Sutka, S. Lagzdina, G. Mezinskis, A. Pludons, I. Vitina, L. Timma. A comparative study of Ni_{0.7}Zn_{0.3}Fe₂O₄ obtained by sol-gel auto-combustion and flash combustion methods. IOP Conf. Series: Materials Science and Engineering 25 (2011) 012019

9. A. Sutka. Metal oxide semiconductor gas sensors. *Latvian Journal of Chemistry*. 2011, 50, 233-241.
10. A. Sutka, M. Stingaciu, G. Mezinskis, A. Lulis. An alternative method to modify the sensitivity of p-type NiFe_2O_4 gas sensor. *Journal of Materials Science*. 2012, 47, pp. 2856–2863.
11. A. Sutka, G. Mezinskis, A. Lulis, D. Jakovlevs. Influence of iron non-stoichiometry on spinel zinc ferrite gas sensing properties. *Sensors & Actuators: B. Chemical*. 2012, 171-172, pp. 204-209.
12. A. Sutka, G. Mezinskis, A. Lulis, M. Stingaciu. Gas sensing properties of Zn-doped p-type nickel ferrite. *Sensors & Actuators: B. Chemical*. 2012, 171-172, pp. 354-360.
13. A. Sutka, G. Mezinskis. Sol-gel auto-combustion synthesis of spinels type ferrite nanomaterials. *Frontiers of Materials Science*, 2012, 6, pp. 128-141.
14. A. Sutka, A. Borisova, J. Kleperis, G. Mezinskis, D. Jakovlevs, I. Juhneva. Effect of nickel addition on colour of nanometer spinel zinc ferrite pigments. *Journal of the Australian Ceramic Society*. 2012, 48, pp. 150-155.
15. A. Sutka, G. Mezinskis. Gas sensitivity of excess-iron Ni-Zn ferrite. *CYSENI 2012*, May 24-25, Kaunas, Lithuania. ISSN 1822-7554
16. A. Sutka, J. Zavickis, G. Mezinskis, D. Jakovlevs, J. Barloti. Ethanol monitoring by ZnFe_2O_4 thin film obtained by spray pyrolysis. *Sensors & Actuators: B. Chemical*. 2012,

Patents

1. A. Sutka, G. Mezinskis. Method for the improvement of gas sensing properties of spinel type ferrite sensors. LV 14372
2. A. Sutka, G. Mezinskis. New spinel type ferrite gas sensor materials. LV 14467

Conference theses

1. A. Sutka, G. Mezinskis, S. Lagzdina. Structural and electric properties of combustion synthesis derived nanocrystalline $\text{Ni}_{0,3}\text{Zn}_{0,7}\text{Fe}_2\text{O}_4$ – investigation of optimal calcination parameters. *Electroceramics 12* (2010), June 13-16, Trondheim, Norway.
2. A. Sutka, G. Mezinskis. Characterization of nano sized Ni-Zn ferrite. *Inter-Academia* (2010), August 9-12, Riga, Latvia.
3. A. Sutka, G. Mezinskis, A. Pludons. Combustion Synthesis, Electrical and Microstructural Properties of $\text{Ni}_{1-x}\text{Zn}_x\text{Fe}_2\text{O}_4$. *Advanced Materials and Technologies* (2010), August 2010, Palanga, Lithuania.
4. S. Lagzdina, A. Sutka. Nanostrukturēta $\text{Ni}_{0,7}\text{Zn}_{0,3}\text{Fe}_2\text{O}_4$ sintēze ar sola-gēla liesmas iniciēšanas un pašaiždegšanās metodēm. 52. RTU studentu zinātniskās un tehniskās konferences materiāli II. pp. 201.

5. A. Sutka, G. Mezinskis, L. Timma, I. Vitina. Electrical and Structural Properties of Nanostructured Stoichiometric and Non-Stoichiometric Ni-Zn Ferrites. BaltSilica 2011: Book of abstracts, 2011, pp. 34-35.
6. G. Mezinskis, L. Grase, I. Buike, A. Pludons, L. Lindina, I. Vitina, A. Sutka. The Evaluation of Illite/Kaolinite Clay Submicrometer Particulate Materials for the Development of Geopolymer Type Solids. BaltSilica2011: Book of abstracts, 2011, pp. 38-39.
7. G. Mezinskis, M. Slesareva, I. Juhnevicā, D. Andersone, M. Karpe, A. Sutka. Photocatalytic Activity of TiO₂ Coatings Deposited on to Porous Silica Glass Fibres. BaltSilica2011: Bookofabstracts, 2011, pp. 70-71.
8. A. Sutka, G. Mezinskis, L. Timma, A. Pludons, S. Lagzdina. Synthesis and Characterization of Nanosized Spinel Ferrites for Gas Sensor Applications. MC10: Conference proceedings, 2011, AT_P172.
9. A. Sutka, G. Mezinskis, A. Lūsis, G. Strikis. Study of impedance properties on non-stoichiometric Ni-Zn ferrite annealed at different temperatures. RTU 52. Starptautiskā zinātniskā konference, 2011, pp. 78.
10. A. Sutka, G. Mezinskis, A. Lūsis. Špineļa tipa ferītu gāzes sensoru raksturošana izmantojot impedances spektraskopiju. Apvienotais pasaules latviešu zinātnieku III kongress, 2011, pp. 116.
11. I. Dirba, A. Sutka, G. Mezinskis, M. Majorovs, J. Kleperis. Synthesis and properties of nano-sized magnetic-hard materials. Institute of Solid State Physics 28th Scientific conference. 2012, pp. 48.
12. A. Knoks, I. Dirba, A. Sutka, M. Majorovs, J. Kleperis, G. Mezinskis. Magnetic and electric field effect on the growth of ferrite films in spray pyrolysis process. Functional Materials and Nanotechnologies. 2012, pp. 176.
13. L. Grinberga, I. Liepina, A. Sutka, J. Kleperis, G. Bajars, G. Mezinskis. Light sensitivity enchase of TiO₂ Thin films with ferrite nanoparticles using multi-source spray-pyrolysis method. Functional Materials and Nanotechnologies. 2012, pp. 177.
14. A. Sutka, G. Mezinskis, A. Lūsis. A route towards more sensitive ZnFe₂O₄ gas sensors. Electroceramics XIII, 2012, pp. 51.